Using lasers to probe the transient light absorption by proteorhodopsin in marine bacterioplankton

Russell A. Desiderio,[1,*] Samuel R. Laney,[1,3] Ricardo M. Letelier,[1] and Stephen J. Giovannoni[2]

[1]College of Oceanic & Atmospheric Sciences, Oregon State University, Corvallis, Oregon 97331, USA
[2]Department of Microbiology, Oregon State University, Corvallis, Oregon 97331, USA
[3]Current address: Biology Department, Woods Hole Oceanographic Institution, Redfield 3-16 MS #32, Woods Hole, Massachusetts 02543, USA

*Corresponding author: desi@coas.oregonstate.edu

Received 7 May 2007; revised 9 September 2007; accepted 27 August 2007; posted 28 August 2007 (Doc. ID 82742); published 9 October 2007

We constructed an experimental apparatus that used lasers to provide the probe beams for measuring the transient absorption kinetics of bacterioplankton that contain proteorhodopsin, a microbial protein that binds retinal and is analogous to animal rhodopsin. With this approach we were able to observe photocycles characteristic of functioning retinylidene ion pumps. Using light from lasers instead of broadband sources as transmittance probe beams can be advantageous when examining optically dense, highly scattering samples such as concentrated microbial cultures. Such a laser-based approach may prove useful in shipboard studies for identifying proteorhodopsin in whole cell suspensions concentrated from seawater.

OCIS codes: 300.6500, 120.6200.

1. Introduction

In transient absorption experiments the transmittance of a probe beam is monitored before and after molecules in the sample absorb photons from a brief, intense flash of light. Changes in transmittance due to this flash indicate the presence of photoactive molecules, and the kinetics of these transients provide insight into the associated photophysics. Transient absorption techniques are commonly used in photobiology to identify the presence of retinal-protein complexes (rhodopsins), pigments that are used for vision but that also have a metabolic function in certain microbes, such as halophilic Archaea. Much of our current understanding of rhodopsin photophysics is derived from studies that employed transient absorption techniques [1,2].

Until recently it has been thought that rhodopsin-mediated light harvesting in microbes occurred in only a narrow range of environments and that the ecological role of this light harvesting was relatively minor. However, gene codings for rhodopsin complexes were identified in marine microbes in 2000 [3], and a marine environmental sample of prokaryotic membranes was shown to exhibit transient absorption traces characteristic of rhodopsin in 2001 [4]. Subsequent DNA studies have catalogued large numbers of microbial genes for rhodopsin in seawater samples worldwide [5]. Since these genes were first identified in marine γ-*Proteobacteria*, rhodopsins from this particular evolutionary line of descent are commonly referred to as "proteorhodopsins," or PRs. PR genes can be expressed in *E. coli* using recombinant genetic methods, and the presence of PR in recombinant bacterial membrane preparations can be confirmed by its characteristic transient absorption signatures [3,4]. Significantly, a gene for PR has been found in SAR11, a marine bacterium that is arguably the most abundant organism in the surface ocean [6,7]. The occurrence of PR genes in SAR11 is particularly noteworthy because a light-driven metabolism in this microbe might alter considerably current perspectives in marine microbial processes and biogeochemistry.

Measurement of transient absorption in optically dense, highly scattering suspensions of microbial cultures involves challenges not encountered when work-

0003-6935/07/297329-08$15.00/0

ing with solutions with negligible scatter or with highly concentrated recombinant membrane preparations. We developed a transient absorption approach for identifying the presence of PR in dense microbial cultures, which we used to collect the first direct evidence that SAR11 cells exhibit PR photocycle kinetics that are characteristic of functioning retinylidene ion pumps [7]. In our approach we used laser beams as probes instead of the more typical broadband (usually incandescent) sources. Lasers are not commonly used as transmittance probes when examining the relatively slow (ms scale) transients of pigments like rhodopsin because of their cost and complexity and because they are monochromatic. However, lasers offer several advantages when working with highly scattering samples. Here we describe this laser-based transient absorption apparatus and demonstrate its ability to detect PR photocycle transient kinetics in cell membrane preparations and in whole-cell suspensions. We show its insensitivity to other non-PR absorbers that may be expected in microbial concentrates that would be collected from natural seawater samples. Finally, we outline potential improvements to this laser-based approach that may increase its sensitivity and broaden its application to shipboard studies of bacterioplankton ecology.

2. Experiment

A. Sample Preparation

Four different microbial samples were prepared that contained PR from SAR11 strain HTCC1062 (High Throughput Culture Collection, Oregon State University): a sample of membranes from recombinant *E. coli* that expressed the HTCC1062 PR gene, and three concentrated cultures of HTCC1062 cells that naturally contain PR [7]. All cultures were grown in 20 liter polycarbonate carboys. Two were grown under a 14:10 hour light–dark cycle of irradiance 24 μmol quanta m^{-2} s^{-1}, and the third was grown in the absence of light. The light-grown cultures were harvested at cell densities of 8.37×10^5 and 1.24×10^6 cells ml^{-1}, and the dark culture was harvested at a density of 1.02×10^6 cells ml^{-1}. All were concentrated using tangential flow filtration, with the retentates spun down and resuspended in sterilized pH 7.9 seawater to a final volume of $\approx$0.35 ml. A dense culture of the marine cyanobacterium *Synechococcus bacillus* was used as a non-PR containing control because this microbe has size and scattering properties roughly similar to those of HTCC1062 but does not contain rhodopsin. All microbial samples were kept on ice until needed for the subsequent spectroscopic measurements.

B. Steady State Spectrophotometry

We measured the spectral transmittance of these five microbial samples using a Cary 300 UV-VIS spectrophotometer (Varian Inc., Palo Alto, CA, USA). Because of the high degree of scattering in these samples, the transmittances that were measured corresponded to the attenuance of the samples and not their absorbance *per se*. These measurements were made in double beam mode using a Suprasil fused silica 1 cm path length cuvette (Hellma 101-QS, Plainview, New York, USA) filled with sterilized pH 7.9 seawater in the reference arm. The volumes of the recombinant PR and *Synechococcus* samples were large enough so that a Hellma 101-QS cell was used for these samples. The small sample volumes of the SAR11 cell resuspensions required the use of a 1 cm path length Spectrosil fused silica fluorescence submicrocuvette (Starna 16.160F-Q-10/Z20, Atascadero CA, USA, nominal volume $\approx$0.16 ml).

A fifth order polynomial was fit to these spectral attenuances to characterize the baseline of their overall spectral scattering and background absorption. These empirical baselines were then subtracted from the spectra in order to check for the existence of small peaks in the attenuance in the wavelength region of expected PR absorption.

C. Transient Spectroscopy

Transient absorption in these samples was measured using a prototype apparatus constructed almost entirely with materials at hand (Fig. 1). In order to demonstrate retinylidene photocycle behavior in SAR11 cultures, we chose two transmittance probe wavelengths that were expected to show opposite behavior with respect to their change in transmission through a PR-containing sample as a function of time after an absorptive pump pulse. These probe beams were conveniently supplied by an argon laser and a helium–neon laser.

One probe beam at 488 nm was supplied by an argon-ion laser (Ar^+, Omnichrome 532, Melles Griot, Carlsbad, CA, USA) running in all-lines mode. A narrowband interference filter (Omega Optical 488DF10) was placed in the Ar^+ beam path to select for the 488 nm laser emission and to reject the other argon laser lines. A 1 m focal length lens was used to shape the beam cross section at the sample into a 1.5 mm diameter circle. A rotatable polarizer provided coarse intensity control of the initially vertically polarized beam. This blue-green beam was transmitted through the red-reflecting dichroic mirror and directed to the sample area.

The second probe beam at 633 nm was supplied by a helium–neon laser (HeNe, Hughes 5000, Melles Griot). A 1 m focal length lens placed in its beam path resulted in an elliptical beam cross section at the sample (vertical major axis of 2 mm, horizontal minor axis of 1 mm). Its intensity was coarsely controlled by a rotatable polarizer followed by a polarizer oriented to pass vertically polarized light. The red 633 nm beam was aligned so that its spot on the dichroic beam splitter was superimposed upon that of the 488 nm beam. The angular orientation of the dichroic beam splitter was adjusted so that the red beam was also superimposed on the blue-green beam in the sample area. In this manner, each of the probe beams served as an alignment beam for the other.

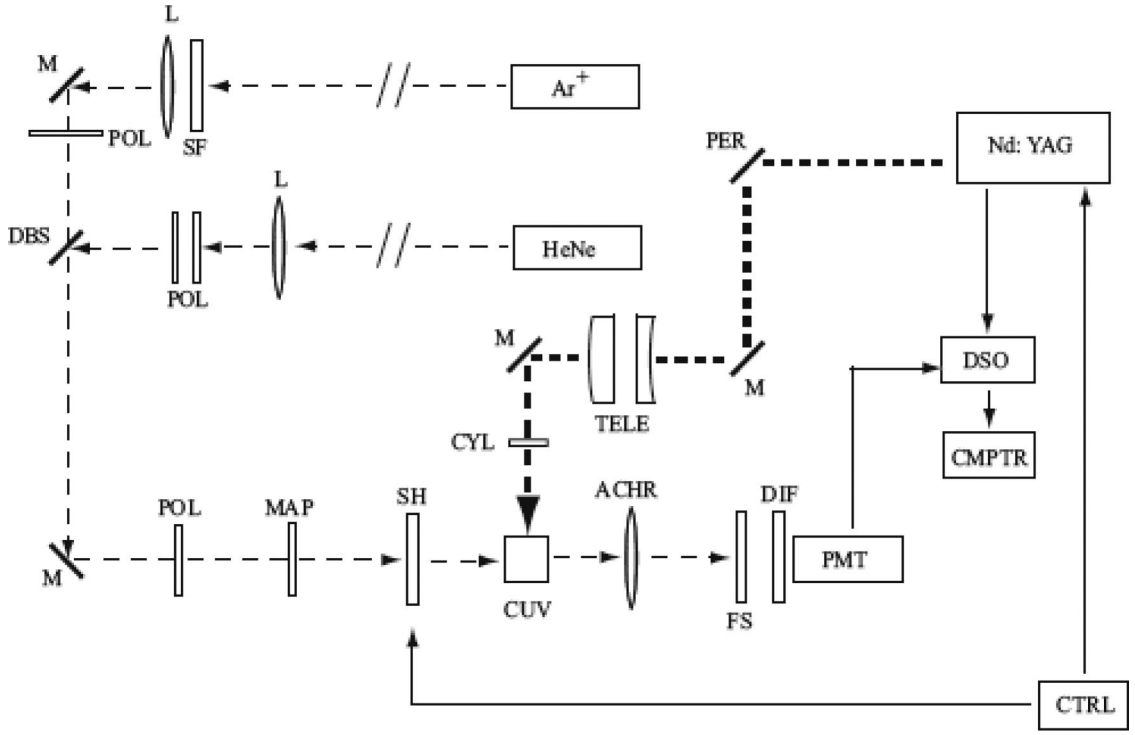

Fig. 1. Schematic of the laser-probe transient absorption apparatus. Green 532 nm pump laser (Nd:YAG), right-skew-angle periscope (PER), mirror (M) beam expanding telescope (TELE), cylindrical lens (CYL), blue 488 nm probe laser (Ar^+), 488 nm spike filter (SF), red 633 nm probe laser (HeNe), 1 m focal length lens (L), polarizer (POL), dichroic beam splitter (DBS), magic angle polarizer (MAP), shutter (SH), fluorescence submicrocuvette (CUV), achromatic collection lens (ACHR), filter sets (FS), diffuser (DIF), photomultiplier tube (PMT), digital storage oscilloscope (DSO), data acquisition computer (CMPTR), and custom-designed system controller (CTRL). The transmission of the filter sets FS, as measured on the Cary spectrophotometer, are as follows: 488 nm FS, 44% T at 488 nm, 25 nm FWHM, out of passband blocking 200–800 nm, OD $>$ 6; 633 nm FS, 48% T at 633 nm, 10 nm FWHM, out of passband blocking 200–800 nm, OD $>$ 6. Solid lines indicate electrical connections. Thin dashed lines indicate probe laser beams; slanted double lines indicate that the lasers were placed as far away from the detection electronics as practicable. Thick dashed lines indicate pump laser beam.

Following the dichroic beam splitter, the probe beams were passed through two polarizers: the first oriented to pass vertically polarized light, and the second oriented at the "magic" angle of 54.7° with respect to the vertical and with respect to the vertically polarized green "pump" beam. This configuration eliminates transient absorption artifacts resulting from molecular motion [1] in samples in which transient intermediates are optically dilute. Typical radiant powers of the probe beams at the samples were 7.5 μW for the 488 nm beam and 3.0 μW for the 633 nm beam.

The cell suspensions were placed in a 1 cm path length Spectrosil fused silica fluorescence submicrocuvette (Starna 16.160F-Q-10/Z20, Atascadero CA, USA) with a 0.2 cm path width and a 0.8 cm path height, resulting in a nominal sample volume of 0.16 ml. Because these were strongly scattering samples, an achromatic lens (50.8 mm diameter, 150 mm focal length) was used to collect and focus the diffuse probe transmittance (typically 0.25 μW) emanating from the cuvette into the transmittance detector assembly. This assembly consisted of a photomultiplier tube (Hamamatsu R374HA) with interference and colored-glass filter sets specific for each probe wavelength and a diffuser inserted in front of its photocathode. In the early stages of these experiments, fluctuations in probe beam intensities were monitored by using glass microscope slides as beam splitters inserted before the dichroic beam splitter to redirect a small fraction of the probe beams to a second reference detector assembly (not included in Fig. 1). The data from the reference detector were collected for instrument characterization purposes but were not used in the following analyses.

Molecular photocycles of rhodopsin in these cell suspensions were induced using the doubled emission at 532 nm from a *Q*-switched Nd:YAG laser (Molectron MY34-10, Coherent Inc., Santa Clara, CA, USA). These "pump" flashes were approximately 5–10 ns in duration. A right-skew-angled periscope was used to bring the pump beam down to probe beam level and to flip its polarization from horizontal to vertical. A telescope and quartz cylindrical lens (focal length 254 mm) were used to expand the beam to a diameter of 12 mm and partially focus it into a horizontal line segment 12 mm long and 2–3 mm high.

Beam overlap at the cuvette position was checked by eye on a white card oriented so that the probe beam(s) hit the card on the front (facing the observer) side and the green beam (with the Nd:YAG laser operating at 10 Hz in "long pulse" mode with the *Q*-switch off) hit the card on the back side. The sam-

ple submicrocuvette was positioned with translation stages so that the probe beams were not clipped on passage through it and so that the green beam completely overlapped the 1 cm path length. System alignment was further checked by measuring the transient signal obtained from a "standard" of recombinant SAR11 PR in a 1 cm fluorometer cuvette.

The pump pulse energy of 10 mJ/pulse was selected by measuring transient absorption signal strengths of a recombinant SAR11 PR sample as a function of pump pulse energy (0.1, 0.3, 1, 3, 10, and 30 mJ/pulse; 16 traces were averaged at each pulse energy). The maximum signal was observed for a pulse energy of 10 mJ; a marked decrease in mean signal strength was observed at 30 mJ/pulse.

Green light from the Nd:YAG laser was occasionally observed at the sample cuvette when the Q switch was closed. Since the Nd:YAG laser system utilized both an oscillator and an amplifier, we were able to eliminate this Q-switch leakage by first setting the oscillator for maximum output and adjusting the amplifier flashlamp energy to produce 30 mJ/pulse in the 532 nm beam. The oscillator flashlamp energy was then decreased until the 532 nm output was 10 mJ/pulse. Under these conditions no Q-switch leakage was observed.

The signal from the transmittance photomultiplier, operating at a photocathode potential of -600 V, was recorded on a digital storage oscilloscope (Tektronix TDS350, Beaverton, OR, USA) and downloaded to a computer following each individual transient trace. The photomultiplier anode output was connected directly to the oscilloscope channel input with a coaxial cable and terminated with a 100 kΩ resistor. To detect the small transmittance transients from our cell suspensions, the probe beam intensity transmitted through the sample was first set to provide a DC signal of about -900 mV by adjusting the polarizers and neutral density filters in the probe beam path. Next, linearity of the detector response was verified by observing the factor of 2 decrease in DC level when a 3 dB neutral density filter was temporarily inserted in front of the detector. The DC level was then set to 0 using the oscilloscope channel's voltage offset, and the channel gain was increased so that small transmittance changes of the order of mV could be detected.

We determined the $1/e$ time response of our apparatus to be 30 μs by observing the decaying exponential signal resulting from monitoring a (much attenuated) 532 nm pump pulse of nominal 5–10 ns duration. Red luminescence excited by the pump pulses was also observed, by eye, from the PR samples and seawater blanks by carefully looking through a Schott long pass OG-570 filter positioned over the fused silica sample cuvettes. As observed on the oscilloscope, this luminescence signal was blocked by a 530 nm interference filter (10 nm bandpass) placed in front of the detector and showed the same exponential decay in time as did that of the pump beam.

The maximum rate of data acquisition was limited by the time required to download one digitized trace from the oscilloscope to the computer (≈22 s). We chose a sample interval of 25 s and used custom-designed electronics to generate the following acquisition sequence. The Nd:YAG flashlamps were continuously triggered at 10 Hz for 23 seconds to maintain the thermal and optical characteristics of the laser cavity. The Q switch was then opened to provide the pump pulse, after which the flashlamps were turned off for 2 seconds during data acquisition to eliminate noise at 10 Hz from discharging the flashlamps. This same circuit operated an electromechanical shutter to shield the sample from the laser probe beams, except for the period from 1 s before to 2 s after the 532 nm pump flash.

Either 32 or 64 of these digitized transient events were collected and averaged at each probe wavelength for each sample. The triggering of each oscilloscope trace was synchronized to the opening of the Nd:YAG Q switch so that the first 20% of the trace occurred before the Q switch was opened; the mean voltage signal for this part of each trace thereby served as its absorption baseline. The voltage values at each digitized point of each individual transient trace were converted to changes in absorbance ΔA relative to the mean voltage of the absorption baseline. The averaged traces were fit to functional forms (see Appendix A) using nonlinear least squares fitting algorithms in Matlab (The Mathworks, Natick, MA, USA). In all of the 633 nm transient traces the first digitized point following the pump flash, whose amplitude was dominated by red luminescence stimulated by the green pump pulse, was removed.

Sterilized seawater blanks and air blanks (empty cuvettes) were analyzed as controls. They exhibited no discernible transmittance transients.

3. Results

A. Steady-State Spectrophotometry

The attenuance spectra of the recombinant *E. coli* with SAR11 PR are shown in Fig. 2(a). In the raw spectrum (solid trace) a small broad peak can clearly be seen in the green region of the spectrum at an OD of 3.6. Subtraction of a quintic baseline reveals a definite peak in the residual spectrum (dashed trace) near 530 nm, the putative absorption peak of recombinant PR [8,9]. The location of this absorption peak corresponds well with the 532 nm wavelength of the doubled Nd:YAG laser that we used to provide the photocycle-inducing pump beam.

Natural SAR11 cells have considerably much less PR than can be expressed in *E. coli* through recombinant techniques. Although the attenuance spectra of the three SAR11 cultures show no obvious peaks [Figs. 2(b)–2(d)], subtraction of a polynomial baseline reveals the presence of small peaks around 530 nm (dashed traces). Applying the same technique to the *Synechococcus* sample [Fig. 2(e)] reveals only the peaks expected for the chlorophyll, carotenoid, and phycobilin pigments that this microbe is known to contain [10,11].

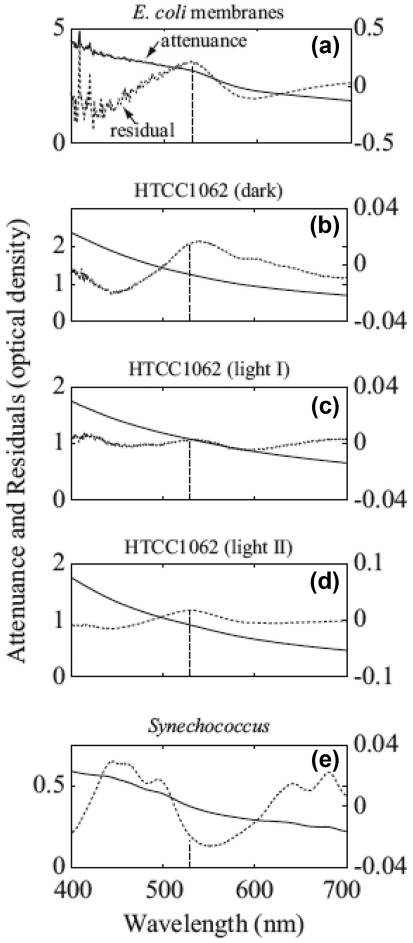

Fig. 2. Static attenuances as a function of wavelength of (a) a membrane preparation of recombinant PR in *E. coli*, (b) a dark-grown HTCC1062 culture, (c) light-grown HTCC1062 culture I, (d) light-grown HTCC1062 culture II, and (e) a control sample of *Synechococcus bacillus*. Solid traces represent total sample attenuance (absorption plus scattering, left ordinate) and dashed traces represent the residual attenuance after subtracting a quintic baseline (right ordinate). Vertical dashed lines are located at 532 nm, the wavelength of the transient-inducing pump beam.

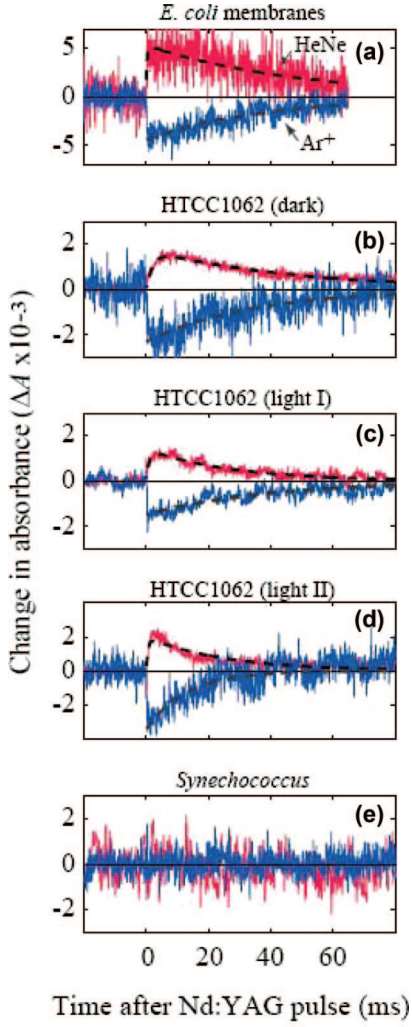

Fig. 3. (Color online) Transient absorption traces for (a) a membrane preparation of recombinant PR in *E. coli*, (b) a dark-grown HTCC1062 culture, (c) light-grown HTCC1062 culture I, (d) light-grown HTCC1062 culture II, and (e) a control sample of *Synechococcus bacillus*. Red (HeNe: 633 nm) absorbance transients are positive, blue (Ar^+: 488 nm) transients are negative. Dashed curves drawn through the data indicate nonlinear regressions (Table 1) to the kinetic model of Appendix A.

B. Transient Absorption Kinetics

All of the PR-containing samples exhibited transient absorption kinetics characteristic of functioning retinylidene ion pumps; the *Synechococcus* control sample exhibited no discernible transients (Fig. 3). The periodic variability apparent in the data is caused by fluctuations of, and interference from, the lasers' power supplies at 60 Hz (Ar^+) and 120 Hz (HeNe). In preliminary experiments, 633 nm data obtained with the HeNe laser showed large amplitude 60 Hz variability that disappeared when the Ar^+ laser was turned off. Similarly, 60 Hz variability in 488 nm data decreased when the Ar^+ laser and power supply were moved as far away from the detection electronics as possible. We were able to further reduce the relative amount of 60 Hz variability by adjustment of the Ar^+ laser's discharge current. The remaining periodic variability in the transmittance signals was not correlated with the intensity of reference signals and is evident in the averaged transient absorption traces.

A simple kinetic model (Appendix A) qualitatively reproduces the transient behavior shown in Fig. 3. Traces of ΔA_{633} generally exhibit a relatively fast exponential rise followed by a slower decay, whereas traces of ΔA_{488} show only an exponential relaxation to the absorption baseline. Fits of this model to the data seem to indicate that statistically significant differences exist among the kinetics of transient absorption and the corresponding time constants of PR photocycles (Table 1). It is particularly interesting to note the similarity in the values obtained for the decay constant τ_O determined for the recombinant PR and dark-grown HTCC1062 samples. However, there is disagreement in the τ_O values determined from ΔA_{488} for the two light cultures; in addition, τ_O values

Table 1. Nonlinear Regression Coefficients and Their 95% Confidence Intervals from Fitting the Data in Fig. 3 to Eqs. (4) and (5) in Appendix A

Sample	C_{633}	τ_M (ms)	τ_O (ms)	C_{488}	τ_O (ms)
Recombinant SAR11 PR in *E. coli* membranes	5.3 ± 0.3	0.3 ± 0.2	49.3 ± 6.1	4.4 ± 0.2	38.5 ± 2.9
HTCC1062 (dark)	1.7 ± 0.1	2.2 ± 0.2	47.3 ± 1.7	2.3 ± 0.1	33.6 ± 2.9
HTCC1062 (light I)	1.4 ± 0.1	1.0 ± 0.2	27.5 ± 1.4	1.5 ± 0.1	39.3 ± 2.4
HTCC 1062 (light II)	1.9 ± 0.1	0.6 ± 0.1	25.7 ± 1.4	3.4 ± 0.2	12.9 ± 1.3

determined from the 633 nm and 488 nm data for a given sample should match within experimental error, which is not observed. These inconsistencies could be due to temperature or pH differences in the samples, photodegradation, or lack of sophistication of our model. In addition, the observed decay rates of the 488 nm traces could be too fast by as much as 5% because the 488 nm probe beams were slightly actinic, and would initiate photocycles in a nonnegligible percentage of PR molecules during the time course of our measurements. Since PR absorbs negligibly at red wavelengths, no such effect would be expected in the 633 nm traces.

The values for the confidence intervals listed in Table 1 should be interpreted as lower limits in that they do not take into account the variability in the absorption baselines occurring after pump pulses, presumably due to thermal effects in our nontemperature regulated samples. Nevertheless, the experimental curves unequivocally demonstrate kinetic behavior characteristic of functioning retinylidene pumps.

4. Discussion

This study demonstrates the effectiveness of using lasers to provide probe beams to measure transient absorption kinetics of microbial rhodopsin. Incandescent lamps are generally preferred as sources for probe beams because of their tunability, but the high spectral radiance of laser beams offers several distinct advantages.

First, lasers can produce more optical power within a narrow bandwidth than broadband lamp sources. Low optical power can be particularly problematic in the blue end of the spectrum when measuring the transmittance of highly scattering samples such as cell suspensions. Furthermore, cell suspensions that are concentrated from large-volume environmental samples (e.g., from seawater) may also contain photosynthetic microbes that absorb considerably in the blue [e.g., Fig. 2(e)]; this occurrence will proportionately weaken the PR-specific transient signal. Future studies that seek to examine PR in cell concentrates from natural seawater will likely need to address this particular issue, whereas typical laboratory examinations of recombinant PR in *E. coli* do not.

A second benefit of using lasers to provide probe beams is that these beams are typically well collimated with narrow beam waists (high étendue). This makes it straightforward to manipulate the beams within the experimental apparatus, particularly for the purpose of maintaining a relatively uniform beam cross section within the sample submicrocuvette. This in turn would facilitate the development of transient absorption systems for shipboard use to examine natural samples at sea.

A third benefit is that laser light is spectrally very narrow, eliminating the need to use a monochromator in the experimental setup. In addition, interference filters with extremely narrow passbands could be used in front of the transmittance detector to more completely reject signal contamination due to broadband luminescence at the probe wavelength at very short times after the excitation flash. We did not exploit the latter advantage in this study because our focus was on detecting transients on the ms time scale in order to identify PR photocycles; the luminescence stimulated by the doubled Nd:YAG laser flashes affected only one time point in the traces shown in Fig. 3. For studies of PR transient absorption at much shorter time scales the use of extremely narrowband filters would provide a considerable improvement in signal quality. For the purposes of simply determining the presence of PR in samples collected from laboratory cultures or environmental samples, however, this signal contamination is negligible.

Our technique of using laser beams as probes in a transient absorption apparatus should be readily applicable to oceanographic field studies to examine the presence of PR in cell suspensions concentrated from natural marine bacterioplankton communities. However, improvements in our current prototypical implementation would be required. First, temperature has a strong effect on PR kinetics in *E. coli* membrane preparations [12], and a similar dependence in live microbes may be expected. A thermostatted cuvette holder could be used to maintain sample temperature to tighter tolerances than was done in this study; an added benefit would be flatter absorption baselines after the pump flash. Second, changes in the pH can also have a strong effect on PR photocycles [13,14], which should also be addressed. Third, AC fluctuations and interference from the lasers' power supplies introduced undesirable variability into our measurements on the time scale of the observed photocycles. Using battery-powered lasers should eliminate this source of variability, but the degree to which such fluctuations occur in other potential laser sources should be investigated before using them in improved designs.

5. Summary

Detecting the presence of PR spectrophotometrically even in a concentrated culture with no outside con-

taminants is problematic. The most direct way to unambiguously detect functioning retinylidene proton pumps in whole cells from microbial cultures, or in concentrated environmental samples, is to observe transient changes in absorption due to the PR photocycle. In this study we demonstrated the feasibility of using lasers as probe beams to measure the transient absorption kinetics of highly scattering, dense microbial suspensions. This laser-based approach provided unambiguous evidence of PR photocycles in both recombinant and naturally expressed PR. Given current technologies, measuring PR transient absorption of bacterioplankton such as SAR11 in the ocean *in situ* (in unconcentrated samples) does not appear to be feasible, because concentrations of PR-containing microbes are too low. It may be possible to develop a shipboard version of our system for use at sea, for which samples could be obtained by using on-board tangential filtration of seawater collected by pumping or by bottle sampling. It would only be necessary to use one red probe beam, most conveniently supplied by a battery-powered laser of suitable wavelength, in such a shipboard system.

Appendix A. A Simple Model of Proteorhodopsin Transient Absorption Kinetics

The PR photocycle can be characterized by kinetic models that describe how unexcited PR molecules, following absorption of light, cycle sequentially through a series of intermediates until they return to their original state. The PR photocycle as observed in various recombinant systems has been investigated by analogy to the photocycle of bacteriorhodopsin [12–14]. We define here a very simplified model to characterize our experimentally observed transients at 488 nm and 633 nm in relation to the time dependent populations of PR and two intermediates, which we will designate as "M" and "O", respectively, also by analogy to the bacteriorhodopsin photocycle.

Two basic assumptions of our model are that (a) an early intermediate ("M") is an unprotonated Schiff base with a blueshifted absorption spectrum, and that (b) a later intermediate ("O") has a strongly redshifted absorption spectrum. These intermediates each have characteristic decay rate constants k_M and k_O respectively, whose inverses are by definition the decay time constants τ_M and τ_O.

$$\mathrm{PR} \overset{k_{\mathrm{fast}}}{\rightarrow} \mathrm{M} \overset{k_M}{\rightarrow} \mathrm{O} \overset{k_O}{\rightarrow} \mathrm{PR}. \tag{1}$$

In this simple model, we assume that the intermediate M does not absorb at 488 nm nor at 633 nm, and that the intermediate O does not absorb at 488 nm but that it is the only component of the photocycle that does absorb at 633 nm. We furthermore assume that PR itself absorbs at 488 nm but does not absorb at 633 nm.

Because the Ar^+ line overlaps the broad absorption band of PR, the transient absorption kinetics of ΔA at 488 nm are modeled simply as the depopulation and repopulation of the unexcited PR state, following the irreversible kinetics expressed by Eq. (1). The PR state is assumed to be instantaneously depopulated by the Nd:YAG laser pulse on the time scale of our experiments [noted in Eq. (1) by the k_{fast} rate constant], so that the repopulation kinetics can be represented by the relationship

$$\Delta A_{488}(t) = -C_{488}\,\frac{\left(k_M e^{-k_O t} - k_O e^{-k_M t}\right)}{k_M - k_O}, \tag{2}$$

where C_{488}, defined to be positive, represents a constant of proportionality dependent upon the absorption strength of PR and the number of PR molecules excited by the pump flash. For our case in which k_M is much greater than k_O, Eq. (2) simplifies to

$$\Delta A_{488}(t) = -C_{488}\left[e^{-k_O t} - (k_O/k_M)e^{-k_M t}\right], \tag{3}$$

which shows that determinations of k_M using these expressions for $\Delta A_{488}(t)$ are not robust because the $e^{-k_M t}$ term is weighted by a factor of the order of (k_O/k_M). Equation (3) further reduces to

$$\Delta A_{488}(t) = -C_{488}e^{-k_O t}, \tag{4}$$

in which the transient absorption at 488 nm is modeled as a simple exponential decay.

Transient absorption kinetics at the HeNe wavelength of 633 nm in this model correspond to the appearance and disappearance of the O intermediate of PR. On the time scale of our experiments, the Nd:YAG pulse effectively converts PR instantaneously into the M state. The M state is depopulated on time scales of the order of ms (τ_M), which is evident as a concurrent increase in the absorption of the subsequent O intermediate at 633 nm at the HeNe probe wavelength. The O intermediate itself depopulates with a longer time constant τ_O of the order of tens of ms,

$$\Delta A_{633}(t) = \frac{k_M}{k_M - k_O}\,C_{633}\left(e^{-k_O t} - e^{-k_M t}\right), \tag{5}$$

where C_{633} represents a (positive) proportionality constant.

The authors would like to thank Bill Hetherington of Oregon State University for providing optical components for this study as well as valuable technical advice, and Joe Nibler and the chemistry department at Oregon State University for allowing us use of their Nd:YAG laser facility. Kevin Vergin and Jang-Cheon Cho supplied the two HTCC1062 culture isolates and the recombinant PR *E. coli*. Partial support for this research was provided by T. J. Cowles.

References

1. R. H. Lozier, "Rapid kinetic optical absorption spectroscopy of bacteriorhodopsin photocycles," Methods Enzymol. **88,** 133–162 (1982).
2. J. K. Lanyi, "Understanding structure and function in the

light-driven proton pump bacteriorhodopsin," J. Struct. Biol. **124,** 164–178 (1998).
3. O. Béjà, L. Aravind, E. V. Koonin, M. T. Suzuki, A. Hadd, L. P. Nguyen, S. B. Jovanovich, C. M. Gates, R. A. Feldman, J. L. Spudich, E. N. Spudich, and E. F. DeLong, "Bacterial rhodopsin: evidence for a new type of phototrophy in the sea," Science **289,** 1902–1906 (2000).
4. O. Béjà, E. N. Spudich, J. L. Spudich, M. Leclerc, and E. F. DeLong, "Proteorhodopsin phototrophy in the ocean," Nature **411,** 786–789 (2001).
5. J. R. de la Torre, L. M. Christianson, O. Béjà, M. T. Suzuki, D. M. Karl, J. Heidelberg, and E. F. DeLong, "Proteorhodopsin genes are distributed among divergent marine bacterial taxa," Proc. Natl. Acad. Sci. USA **100,** 12830–12835 (2003).
6. M. S. Rappé, S. A. Connon, K. L. Vergin, and S. J. Giovannoni, "Cultivation of the ubiquitous SAR11 marine bacterioplankton clade," Nature **418,** 630–633 (2002).
7. S. J. Giovannoni, L. Bibbs, J.-C. Cho, M. D. Stapels, R. Desiderio, K. L. Vergin, M. S. Rappé, S. Laney, L. J. Wilhelm, H. J. Tripp, E. J. Mathur, and D. F. Barofsky, "Proteorhodopsin in the ubiquitous marine bacterium SAR11," Nature **438,** 82–85 (2005).
8. B. R. Kelemen, M. Du, and R. B. Jensen, "Proteorhodopsin in living color: diversity of spectral properties within living bacterial cells," Biochim. Biophys. Acta **1618,** 25–32 (2003).
9. D. Man, W. Wang, G. Sabehi, L. Aravind, A. F. Post, R. Massana, E. N. Spudich, J. L. Spudich, and O. Béjà, "Diversification and spectral tuning in marine proteorhodopsins," EMBO J. **22,** 1725–1731 (2003).
10. M. Stomp, J. Huisman, F. de Jongh, A. J. Veraart, D. Gerla, M. Rijkeboer, B. W. Ibelings, U. I. A. Wollenzien, and L. J. Stal, "Adaptive divergence in pigment composition promotes phytoplankton biodiversity," Nature **432,** 104–107 (2004).
11. K. S. Rowan, *Photosynthetic Pigments of Algae* (Cambridge University Press, 1989).
12. G. Váró, L. S. Brown, M. Lakatos, and J. K. Lanyi, "Characterization of the photochemical reaction cycle of proteorhodopsin," Biophys. J. **84,** 1202–1207 (2003).
13. A. K. Dioumaev, L. S. Brown, J. Shih, E. N. Spudich, J. L. Spudich, and J. K. Lanyi, "Proton transfers in the photochemical reaction cycle of proteorhodopsin," Biochemistry **41,** 5348–5358 (2002).
14. R. A. Krebs, A. Alexiev, R. Partha, A. M. DeVita, and M. S. Braiman, "Detection of fast light-activated H^+ release and M intermediate formation from proteorhodopsin," BMC Physiol. 2:5 (2002).